

UCLA

UCLA Previously Published Works

Title

Quantitative 4D imaging of biomechanical regulation of ventricular growth and maturation.

Permalink

<https://escholarship.org/uc/item/2v1018dp>

Authors

Cho, Jae

Poon, Mong

Zhu, Enbo

et al.

Publication Date

2023-06-01

DOI

10.1016/j.cobme.2022.100438

Peer reviewed



Published in final edited form as:

Curr Opin Biomed Eng. 2023 June ; 26: . doi:10.1016/j.cobme.2022.100438.

Quantitative 4D imaging of biomechanical regulation of ventricular growth and maturation

Jae Min Cho^{1,2,*}, Mong Lung Steve Poon^{4,*}, Enbo Zhu^{1,2,*}, Jing Wang³, Jonathan T. Butcher^{4,**}, Tzung Hsiai^{1,2,3,**}

¹Division of Cardiology, Department of Medicine, David Geffen School of Medicine, UCLA

²Department of Medicine, Greater Los Angeles VA Healthcare System

³Department of Bioengineering, UCLA

⁴Nancy E. and Peter C. Meinig School of Biomedical Engineering, Cornell University

Abstract

Abnormal cardiac development is intimately associated with congenital heart disease. During development, a sponge-like network of muscle fibers in the endocardium, known as trabeculation, becomes compacted. Biomechanical forces regulate myocardial differentiation and proliferation to form trabeculation, while the molecular mechanism is still enigmatic. Biomechanical forces, including intracardiac hemodynamic flow and myocardial contractile force, activate a host of molecular signaling pathways to mediate cardiac morphogenesis. While mechanotransduction pathways to initiate ventricular trabeculation is well studied, deciphering the relative importance of hemodynamic shear vs. mechanical contractile forces to modulate the transition from trabeculation to compaction requires advanced imaging tools and genetically tractable animal models. For these reasons, the advent of 4-D multi-scale light-sheet imaging and complementary multiplex live imaging via micro-CT in the beating zebrafish heart and live chick embryos respectively. Thus, this review highlights the complementary animal models and advanced imaging needed to elucidate the mechanotransduction underlying cardiac ventricular development.

** Corresponding authors: Jonathan T. Butcher, Nancy E. and Peter C. Meinig School of Biomedical Engineering, Cornell University; Tzung Hsiai, Division of Cardiology, Department of Medicine, David Geffen School of Medicine at University of California Los Angeles, CA 90095, USA, Thsiai@mednet.ucla.edu.

* Authors contributed equally.

Author contributions

JMC, MP, EZ, & JW prepared visualizations; JMC, MP, and EZ contributed to the first draft; JB & TZ edited the manuscript, and TZ was responsible for overall coordination. All authors read and approved the final manuscript.

Publisher's Disclaimer: This is a PDF file of an unedited manuscript that has been accepted for publication. As a service to our customers we are providing this early version of the manuscript. The manuscript will undergo copyediting, typesetting, and review of the resulting proof before it is published in its final form. Please note that during the production process errors may be discovered which could affect the content, and all legal disclaimers that apply to the journal pertain.

Declaration of competing interest

The authors declare that they have no known competing financial interests or personal relationships that could have appeared to influence the work reported in this article.

Declaration of interests

The authors declare that they have no known competing financial interests or personal relationships that could have appeared to influence the work reported in this paper.

Keywords

Hemodynamics; Trabeculation; Light-sheet; Micro-CT; Ultrasound

1. Introduction

Left ventricular non-compaction cardiomyopathy (LVNC) is a congenital heart disease of non-compacted endomyocardium known as *spongy* myocardium, or hypertrabeculation [1]. Individuals with LVNC carry a high-risk for developing malignant arrhythmias, thromboembolic events, and ventricular dysfunction [2]. Failure to arrest the myocardial proliferation is implicated in ventricular hypertrabeculation, resulting in a reduction in ventricular compliance; and, subsequently, ventricular diastolic dysfunction [3]. Studies have linked left ventricular non-compaction with the autosomal dominant inherited disorders, and mutation in Notch signaling pathway is implicated in defective trabeculation and ventricular non-compaction cardiomyopathy (NCC) [4].

A significant reduction in trabeculation is associated with a deficiency in ventricular compact zone or known as the hypoplastic heart syndrome, whereas hypertrabeculation is closely associated with LVNC [5]. The former predisposes patients to developing heart failure mainly due to systolic dysfunction with depressed ventricular ejection fraction (HFrEF), whereas the latter leads to diastolic heart failure with preserved EF (HFpEF) [6]. LVNC is the third most common cardiomyopathy after dilated and hypertrophic cardiomyopathy in the pediatric population. During heart development, trabeculation facilitates oxygenation and nutritional delivery to the myocardium to enhance cardiac contractile function [7]. Thus, elucidating the mechanotransduction mechanism underlying cardiac trabeculation, along with developing advanced imaging and genetic animal models, hold promises for identifying the therapeutic targets.

2.1. The role of Notch signaling in trabecular organization

Notch receptor-ligand interaction is a well-recognized signaling pathway to mediate cardiomyocyte proliferation and differentiation [8]. Mutations in Notch pathway regulator, mind bomb homolog 1 (MIB1), which encodes an E3 ubiquitin ligase to promote endocytosis of the Notch ligands Delta or Jagged, is associated with reduced Notch activity, and the reduced Notch effectors Hey1, Hey 2, and target genes are implicated in LVNC in the autosomal-dominant pedigrees [8]. Notch activation by Delta-like 1 (Dll1) or Delta-like 4 (Dll4) in the endocardial endothelial cells results in transcription of Ephrin B2 to regulate Neuroregulin (Nrg1) [8]. In parallel, Notch signaling activates bone morphogenetic protein 10 (BMP10) expression, and both Nrg1 and BMP 10 activate myocardial ErbB2/4 to promote myocyte differentiation and proliferation [8]. In mice, deficiency in either Nrg1 or ErbB2/4 leads to hypoplastic ventricular walls lacking normal trabeculation [9], whereas *BMP10* overexpression in the myocardium promotes hypertrabeculation in the Nkx2.5-myocardial specific knockout [10]. In Zebrafish, endocardial Nrg1-mediated EbrB2/4 regulates cardiomyocyte delamination to initiate ventricular trabeculation [11]. Complementing findings in early trabeculation, notch activity is implicated in both the growth and maturation of trabeculae, and myocardium compaction in chick embryos

(Fig. 4m). Furthermore, Notch1 is considered as a “double-edged sword” in regulating trabeculation; that is, both depletion and overactivation of Notch1 is reported to develop NCC [1], implicating the roles of lateral activation vs. inhibition in modulating trabecular formation. While biomechanical forces; namely, myocardial contraction and intracardial hemodynamic shear stress, are closely linked with cardiac morphogenesis, it remains experimentally challenging to decipher the relative contribution of these two forces to coordinate trabecular initiation and organization. In this context, developing advanced imaging tools, along with the genetically tractable animal models, is conducive to elucidating the mechanotransduction mechanisms underlying trabecular organization for optimal contractile function.

2.2. Myocardial contractile force differentially activates endocardial vs. myocardial Notch signaling

The Notch pathway is subject to numerous levels of molecular regulation, including positive and negative feedback loops or lateral activation vs. inhibition [12]. The precise outcome of Notch activation is often sensitive to cell-cell interaction during developmental stages [8]. In the classic Notch “*lateral inhibition*” model, cells committed to a given fate inhibit their neighbors from adopting the same fate. The Notch activity is localized by its tissue-specific ligand expression (Dll1 and Dll4 vs. Jag1 and Jag2); namely, Dll1/Dll4 are expressed in the ventricular endocardium or endothelium [8], and Jagged1/2 are expressed in the cardiomyocytes [13]. Han and Chi *et al.* reported that myocardial Notch ligand Jag2b inhibits the neighboring myocardial ErbB2 signaling to prevent cardiomyocyte sprouting and trabeculation [14], whereas endothelial-specific Notch ligand Dll1/Dll4 activates Nrg1 signaling to promote myocardial ErbB2/4 activation and subsequent myocardial differentiation and proliferation to form trabeculae in mouse [15].

In zebrafish embryonic hearts [16], intracardiac hemodynamic shear force induces endocardial Notch-Nrg1-ErbB2 signaling to initiate trabeculation [17]. Whether hemodynamic shear and myocardial contractile forces coordinate Notch signaling-mediated trabecular organization; specifically, ridge and groove formation, remains elusive [18]. While hemodynamic force induces endocardial Delta-Notch interaction to activate the neighboring ErbB2 signaling, myocardial contractile force induces myocardial Jag2b-Notch to inhibit the neighboring ErbB2 signaling, the precise Mechanotransduction mechanisms to orchestrate the trabecular organization needed to optimize ventricular structure and function remain to be explored.

2.3. Mouse (*Mus musculus*), Chicken (*Gallus domesticus*), and zebrafish (*Danio rerio*) systems to investigate developmental cardiac biomechanics

The mouse, chicken, and zebrafish models are well-established genetic systems to study cardiac development and disease. Recent mouse studies corroborate that Notch1 [1] gene modulate cardiac trabeculation. Although microinjection can be applied to embolize the mouse fetal left atrium as a means of recapitulating the congenital heart disease [19], and genetic manipulation can be performed to demonstrate the hypoplastic left heart syndrome (HLHS) in mouse cardiac development studies [20], the multigenic etiology and genetic heterogeneity of mouse model along with its variable expressivity and incomplete

penetrant complicated the genetic and epigenetic study [21]. In addition, it is experimentally challenging to investigate cardiac biomechanics in the individual fetuses inside the placenta of the pregnant mouse. For this reason, most of the investigators have resorted to chicken and zebrafish models.

Chick embryo (*Gallus gallus*) is a classical model for biomechanics during cardiac development because of its 4-chamber heart and the ease of surgical manipulation in the yolk sac [22]. The developmental stages of four-chamber heart resemble those of human cardiac physiology. In the era of precision medicine and genomics, the transcriptomic atlas in chick embryo heart was recently reported to reveal different stages of heart development (at 4, 7, 10, 14 days) using single cell RNA sequencing (scRNA-seq) and spatial transcriptomics [23] that offer an unbiased genetic database for studying the early developmental stages of chick hearts. The chick embryo is highly amenable to experimental manipulation, real-time imaging, and surgical intervention [23]. To study the effects of intracardiac hemodynamics on ventricular trabeculation and valve formation, investigators can perform vitelline vein ligation, outflow tract bending, right atrial ligation, or left atrial ligation in a single chick embryo to alter the cardiac flow pattern (Table 1) [22, 24]. The advantage of using chicken embryos resides in its physical accessibility to the cardiovascular structure for visualization and surgical procedure to change the right and left ventricular hemodynamics, otherwise experimentally challenging in mouse. Furthermore, advances in genome editing technologies, particularly CRISPR-Cas 9 system, have opened increasing opportunities to systemically interrogate the genetic elements and variations in chicken embryo [25].

Zebrafish (*Danio rerio*) is a widely recognized model for developmental biology. Diverging from mammalian ancestry 450 million years ago, zebrafish possess the essential common anatomy of humans [26]. Despite having a two-chamber heart and a lack of pulmonary vascular system, the adult zebrafish electrocardiogram (ECG) is analogous to that of humans [27, 28]. Its small size and fecundity facilitate genetic perturbations to enable high throughput genetic, epigenetic, and pharmaceutical studies [29]. Despite the technical limitations to evaluate the biomechanical forces in mammalian development, zebrafish embryos are optically transparent and genetically tractable for investigating cardiac morphogenesis [30]. Thus, zebrafish model is uniquely conducive to elucidating the coordination of myocardial contractility and intracardiac shear stress, and to perform the gain- and loss-of-function analyses (Table 1) [27]. Overall, both zebrafish and chick models are complementary to elucidate the interplay between genetic and mechanical interaction underlying myocardial trabeculation and compaction [27].

2.4. Trabeculation Engenders Local Hemodynamic Gradients

In the adult zebrafish model of myocardial injury and regeneration, ultrasonic transducers (by applying the B-mode imaging at 75 MHz and pulsed-wave Doppler at 45 MHz) was used to measure early passive filling ([E]-wave velocity) and active filling (atrial [A]-wave velocity) during diastole (Fig. 1a–d) [29]. E/A ratio is > 1 for normal diastolic function, whereas $E/A < 1$ indicates diastolic dysfunction from hyper-trabeculation or LVNC [29]. As a corollary, *in silico* analysis revealed that the elevated oscillatory shear index (OSI)

in trabecular ridges increases endocardial kinetic energy (KE) dissipation that modulates ventricular contractile function and remodeling [31]. The 4-D computational fluid dynamics (CFD) simulations showed that pulsatile flow across the AV valve produces high KE impacting the endocardium, followed by increased KE dissipation (Fig. 1e). Both inhibitions of atrial contraction (*wea* mutant) and reduction in viscosity (*gata1a* Morpholino) reduced the magnitude of KE (Figs. 1f), and subsequently, reduced KE dissipation throughout the cardiac cycle (Figs. 1g). Notably, the *wea* mutation resulted in a reduction in both KE and energy dissipation (Figs. 1f–g) [31]. Complementarily, it is noteworthy that 4-D high-frequency ultrasonic scans have also been utilized to determine the hemodynamics and cardiac functions in chick embryo despite lacking comprehensive characterization of trabecular energetics to date [32]. Furthermore, a hybrid laser system, namely, the light-sheet and light-field imaging can be custom-built to decouple hemodynamic shear from myocardial contractile forces to study the trabecular ridge and groove formation [33].

2.5. A Hybrid System to Integrate Light-Sheet with the Light-Field System

2.5.1. Multi-Scale Light-Sheet Fluorescent Microscope—Three imaging modalities are commonly utilized to study the tissue development, injury, and regeneration: 1) laser-scanning confocal microscopy (LSCM), 2) spinning-disk confocal microscopy (SDCM), and 3) light-sheet fluorescence microscopy (LSFM) [34]. LSCM and SDCM are both pinhole-based fluorescence microscopy. SDCM increased the scanning speed but sacrificed the axial resolution due to the pinhole crosstalk. Compared with LSCM and SDCM, LSFM provides higher imaging acquisition speed, lower phototoxicity and deep tissue penetration, rendering it unique for 3D imaging of the larger tissues. A multi-scale LSFM system enables the dual-illumination lenses to reshape a thin laser-sheet (1–10 μm in thickness), allowing for rapid scanning across a sample of interest while the detection lens orthogonally collects the imaging data (Fig. 2a–k) [35].

The LSFM system can be custom-built for rapid data acquisition, followed by a post-image synchronization algorithm for 4-D registration and reconstruction [36]. This system provides high spatiotemporal resolution and minimal photo-bleaching, allowing for *in vivo* visualization of the developing hearts in the zebrafish embryos ($\sim 0.4 \times 0.5 \times 0.6 \text{ mm}^3$ at ~ 30 sec) [35], *ex vivo* interrogation of the neonatal and adult mouse hearts ($\sim 8 \times 8 \times 10 \text{ mm}^3$ at ~ 120 sec), and visualization of AV valve leaflet excursion at 5 days post fertilization (dpf) (Fig. 2l–n) [37].

To achieve high-throughput volumetric imaging, investigators have further developed a non-axially-scanned sub-voxel LSFM (SV-LSFM) system [38], allowing for the acquisition of giga voxels/min (Fig. 2o–p) [39]. This super-resolution strategy generates additional photons to excite 3–4 fluorescent-labeled structures in the sample. The thickness of the light-sheet (1–10 μm) determines the depth of the optical section viewed by the camera. By using a graphic processing unit (GPU)-based computation, we resolved the neural muscular junction (Fig. 2o) and the intact neonatal mouse heart (Fig. 2p).

2.5.2. Multi-view Light-Sheet Fluorescent Microscope for super-resolution imaging—Zebrafish embryos and larvae provide optical transparency until 5 dpf, after

which they gradually develop pigmentation and tissue growth. This opacity renders it challenging to further capture cardiac development. Efforts have been devoted to genetically engineer the less opaque zebrafish models, such as the *casper* line [40]. Alternatively, phenylthiourea (PTU) can be used to block pigmentation and to improve optical transparency [41]. However, opacity may remain persistent, as the organs/tissues grow. To overcome deep tissue penetration, investigators have developed a multi-view LSFM combined with SV-LSFM. This multi-view strategy is accomplished by registering, weighting, and fusing a number of image stacks recorded under different views and finally recovers a stack that shows complete signals with improved axial resolution [38]. With such a combination, investigators can achieve complete imaging of scattering samples and establish an isotropic resolution of $\sim 1.6 \mu\text{m}$ (compared with the original $\sim 6.5 \mu\text{m}$ and $26 \mu\text{m}$) throughout a volume of $>100 \text{mm}^3$.

2.5.3. Multiplex imaging of intracardiac flow dynamics and myocardial contractile vectors—The multiplex imaging advances our capacity to elucidate cardiac structure and function in zebrafish. For example, one can combine a view-channel-depth (VCD) neural network with light-field microscopy and simultaneously image intracardiac flow dynamics and myocardial contractile vectors in a beating zebrafish heart at a single-cell level (Fig. 2q–u) [36, 42]. This VCD-LSFM yields artifact-free 3-D image sequences with uniform spatial resolution and high-video-rate reconstruction up to 200 Hz volumetric imaging rates. One can also integrate light-field microscopy with LSFM and couple with a retrospective gating method, to simultaneously access myocardial contraction and intracardiac blood flow at 200 volumes per second. This approach captures the time-dependent tracking of the individual blood cells and the differential rates of segmental wall displacement during a cardiac cycle [43].

2.5.4 Live Micro-CT to quantify dynamic trabeculation and compaction in the chick model—Micro-computed tomography (micro-CT) has emerged as a promising imaging tool to study ventricular trabecular growth and maturation in response to changes in ventricular preload or afterload in the chick model. By detecting the attenuation of x-ray passing through a sample, micro-CT enables non-destructive, high-resolution visualization of the 3-D microstructure of perfused 4-chamber hearts (Fig. 3a–d) [44]. The micro-CT images, along with ultrasound-measured blood flow rates, can also be integrated into computational fluid dynamic model to simulate the cardiac hemodynamics during normal and diseased heart development (Fig. 3e–g) [16]. This allows the measurement of the 3-D and 4-D blood flow velocities and the distribution of wall shear stress on the endocardium, facilitating the interrogation of clinically relevant ventricular malformation (Fig. 3h–j) [45]. To further enhance the spatial and temporal resolution of micro-CT, investigators have developed an artifact-free 3-D cardiac imaging modality by tracking the heartbeat signal into a tunable gating trigger using Eulerian video magnification (Fig. 4a–f) [46]. Prospective gated 3-D reconstruction of the HH34 embryos (<2 hrs contrast incubation) revealed clear 3-D cardiac structures at both systole and diastole, allowing the precise monitoring of ventricular trabecular dynamics and myocardial energetics (Fig. 4g–l).

3. Conclusion and Perspective

To explore therapeutic targets for LVNC, investigators have focused on how biomechanical forces, especially intracardiac hemodynamic flow, induce endocardial trabeculation in the developing heart. In preclinical study of cardiac trabeculation, both mouse and chick embryos are complementary models for their genetically tractable systems and developmental states. Computational simulation from pulsed wave (PW) doppler images can reconstruct the endocardial hemodynamics and ventricular kinetic energy (KE). To capture biomechanical forces-mediated cardiac trabeculation, investigators have demonstrated a hybrid system to integrate light-sheet with the light-field system, along with the multi-scale light-sheet fluorescent microscope, multiplex imaging. To capture the 4-chamber chick heart, investigators have developed the micro-CT to enable detection of hemodynamics and non-invasively overlaying functional and molecular or phenotypic signatures in the same chick during the cardiac trabeculation in the embryonic chick heart.

Nevertheless, new technical break-through is warranted to further advance the study of cardiac morphogenesis into the later periods where clinically significant malformations emerge. Despite the advent in light-sheet and light-field imaging, tissue opacity limits our capacity to acquire trabeculation imaging in late stage of cardiac development. Furthermore, integrating structural and functional changes with the developmental genomics, in addition to Notch1 signaling pathway, is essential to provide both holistic and unbiased approaches to address the temporal and spatial variations of biomechanical forces, along with the dynamic changes in genetic or transcriptional factors. While a recent study revealed the transcriptomic atlas during cardiac development using a combination of scRNA-seq and spatial transcriptomics in chick embryo [23], acquiring sufficient cells counts for scRNA-seq analyses remains an experimental challenge. New advances in RNA *in situ* hybridization transforms molecular detection with morphological context have emerged to enable spatial and temporal correlation between mechanical forces and transcriptomics [47]. In summary, integration of advanced imaging for deep tissue penetration with spatial and temporal transcriptomics and bioinformatics [48] paves the way to advance the field of mechanobiology in cardiac development.

Acknowledgments

We would like to acknowledge our funding support from the National Heart Lung, and Blood Institute: R01 HL129727 (TKH), R01 HL 159970 (TKH), R01 HL165318 (TKH), R01 HL160028 (JTB). JTB is also supported by a SVD grant from Additional Ventures.

References

- [1]. Del Monte-Nieto G, Ramialison M, Adam AAS, Wu B, Aharonov A, D'Uva G, Bourke LM, Pitulescu ME, Chen H, de la Pompa JL, Shou W, Adams RH, Harten SK, Tzahor E, Zhou B, Harvey RP, Control of cardiac jelly dynamics by NOTCH1 and NRG1 defines the building plan for trabeculation, *Nature* 557(7705) (2018) 439–445. [PubMed: 29743679]
- [2]. MacGrogan D, Munch J, de la Pompa JL, Notch and interacting signalling pathways in cardiac development, disease, and regeneration, *Nat Rev Cardiol* 15(11) (2018) 685–704. [PubMed: 30287945]
- [3]. Halaney DL, Sanyal A, Nafissi NA, Escobedo D, Goros M, Michalek J, Acevedo PJ, Perez W, Patricia Escobar G, Feldman MD, Han HC, The Effect of Trabeculae Carneae on Left Ventricular

Diastolic Compliance: Improvement in Compliance With Trabecular Cutting, *J Biomech Eng* 139(3) (2017).

- [4]. Luxan G, D'Amato G, MacGrogan D, de la Pompa JL, Endocardial Notch Signaling in Cardiac Development and Disease, *Circ Res* 118(1) (2016) e1–e18. [PubMed: 26635389]
- [5]. Zhang W, Chen H, Qu X, Chang CP, Shou W, Molecular mechanism of ventricular trabeculation/compaction and the pathogenesis of the left ventricular noncompaction cardiomyopathy (LVNC), *Am J Med Genet C Semin Med Genet* 163C(3) (2013) 144–56. [PubMed: 23843320]
- [6]. Brescia ST, Rossano JW, Pignatelli R, Jefferies JL, Price JF, Decker JA, Denfield SW, Dreyer WJ, Smith O, Towbin JA, Kim JJ, Mortality and sudden death in pediatric left ventricular noncompaction in a tertiary referral center, *Circulation* 127(22) (2013) 2202–8. [PubMed: 23633270]
- [7]. Sedmera D, Pexieder T, Vuillemin M, Thompson RP, Anderson RH, Developmental patterning of the myocardium, *Anat Rec* 258(4) (2000) 319–37. [PubMed: 10737851]
- [8]. High FA, Epstein JA, The multifaceted role of Notch in cardiac development and disease, *Nat Rev Genet* 9(1) (2008) 49–61. [PubMed: 18071321]
- [9]. Lai D, Liu X, Forrai A, Wolstein O, Michalick J, Ahmed I, Garratt AN, Birchmeier C, Zhou M, Hartley L, Robb L, Feneley MP, Fatkin D, Harvey RP, Neuregulin 1 sustains the gene regulatory network in both trabecular and nontrabecular myocardium, *Circ Res* 107(6) (2010) 715–27. [PubMed: 20651287]
- [10]. Pashmforoush M, Lu JT, Chen H, Amand TS, Kondo R, Pradervand S, Evans SM, Clark B, Feramisco JR, Giles W, Ho SY, Benson DW, Silberbach M, Shou W, Chien KR, Nkx2-5 pathways and congenital heart disease; loss of ventricular myocyte lineage specification leads to progressive cardiomyopathy and complete heart block, *Cell* 117(3) (2004) 373–86. [PubMed: 15109497]
- [11]. Liu J, Bressan M, Hassel D, Huisken J, Staudt D, Kikuchi K, Poss KD, Mikawa T, Stainier DY, A dual role for ErbB2 signaling in cardiac trabeculation, *Development* 137(22) (2010) 3867–75. [PubMed: 20978078]
- [12]. Bray SJ, Notch signalling: a simple pathway becomes complex, *Nat Rev Mol Cell Biol* 7(9) (2006) 678–89. [PubMed: 16921404]
- [13]. Niessen K, Karsan A, Notch signaling in cardiac development, *Circ Res* 102(10) (2008) 1169–81. [PubMed: 18497317]
- [14]. Han P, Bloomekatz J, Ren J, Zhang R, Grinstein JD, Zhao L, Burns CG, Burns CE, Anderson RM, Chi NC, Coordinating cardiomyocyte interactions to direct ventricular chamber morphogenesis, *Nature* 534(7609) (2016) 700–4. [PubMed: 27357797]
- [15]. Priya R, Allanki S, Gentile A, Mansingh S, Uribe V, Maischein HM, Stainier DYR, Tension heterogeneity directs form and fate to pattern the myocardial wall, *Nature* 588(7836) (2020) 130–134. [PubMed: 33208950] ** In cardiac trabeculation process, cardiomyocytes sequentially: 1) are proliferated and crowded by *Erb2*; 2) are exposed to tension heterogeneity which leads to delamination; and 3) are segregated compact and trabecular layers. Importantly, Notch signaling activates in the next to the delaminated cardiomyocytes and prevents delamination in the cardiomyocytes, whereas trabecular layer triggers actomyosin contractility.
- [16]. Foo YY, Motakis E, Tiang Z, Shen S, Lai JKH, Chan WX, Wiputra H, Chen N, Chen CK, Winkler C, Foo RSY, Yap CH, Effects of extended pharmacological disruption of zebrafish embryonic heart biomechanical environment on cardiac function, morphology, and gene expression, *Dev Dyn* 250(12) (2021) 1759–1777. [PubMed: 34056790] * A pharmacological strategy to inhibition of biomechanical force by 2,3-butanedione monoxime (BDM) results in malformation of trabeculation along with *notch1* and *erbb4a* in zebrafish. This paper used combination of transcriptomics and computational fluid dynamics by line-scan focal modulation microscopy.
- [17]. Masumura T, Yamamoto K, Shimizu N, Obi S, Ando J, Shear stress increases expression of the arterial endothelial marker *ephrinB2* in murine ES cells via the VEGF-Notch signaling pathways, *Arterioscler Thromb Vasc Biol* 29(12) (2009) 2125–31. [PubMed: 19797707]
- [18]. Samsa LA, Givens C, Tzima E, Stainier DY, Qian L, Liu J, Cardiac contraction activates endocardial Notch signaling to modulate chamber maturation in zebrafish, *Development* 142(23) (2015) 4080–91. [PubMed: 26628092]

- [19]. Rahman A, DeYoung T, Cahill LS, Yee Y, Debebe SK, Botelho O, Seed M, Chaturvedi RR, Sled JG, A mouse model of hypoplastic left heart syndrome demonstrating left heart hypoplasia and retrograde aortic arch flow, *Dis Model Mech* 14(11) (2021).
- [20]. Lu P, Wang P, Wu B, Wang Y, Liu Y, Cheng W, Feng X, Yuan X, Atteya MM, Ferro H, Sugi Y, Rydquist G, Esmaily M, Butcher JT, Chang CP, Lenz J, Zheng D, Zhou B, A SOX17-PDGFB signaling axis regulates aortic root development, *Nat Commun* 13(1) (2022) 4065. [PubMed: 35831318] ** Aortic root endothelial SRY-byx 17 (SOX17), a transcription factor to regulate Notch1 signaling, deficiency results in aortic root malformation followed by non-coronary leaflets and mispositioned left coronary ostium in mouse. Mechanistically, defective SOX17 hinders the transcriptional interaction between SOX17 and PDGF.
- [21]. Gabriel GC, Yagi H, Xu X, Lo CW, Novel Insights into the Etiology, Genetics, and Embryology of Hypoplastic Left Heart Syndrome, *World J Pediatr Congenit Heart Surg* 13(5) (2022) 565–570. [PubMed: 36053093]
- [22]. Alser M, Shurbaji S, Yalcin HC, Mechanosensitive Pathways in Heart Development: Findings from Chick Embryo Studies, *J Cardiovasc Dev Dis* 8(4) (2021).
- [23]. Mantri M, Scuderi GJ, Abedini-Nassab R, Wang MFZ, McKellar D, Shi H, Grodner B, Butcher JT, De Vlaminc I, Spatiotemporal single-cell RNA sequencing of developing chicken hearts identifies interplay between cellular differentiation and morphogenesis, *Nat Commun* 12(1) (2021) 1771. [PubMed: 33741943] ** This paper mapped cellular lineage of developing heart using a hybrid strategy, combination between scRNAseq and spatial transcriptomics using anchor-based methods in different heart development stages: day 4 (early chamber development), day 7 (early 4 chamber development), day 10 (mid 4 chamber development) and day 14 (late 4 chamber development). Significantly, this study revealed that thymosin beta-4 is ubiquitously expressed during development of cardiac chambers.
- [24]. Gould RA, Yalcin HC, MacKay JL, Sauls K, Norris R, Kumar S, Butcher JT, Cyclic Mechanical Loading Is Essential for Rac1-Mediated Elongation and Remodeling of the Embryonic Mitral Valve, *Curr Biol* 26(1) (2016) 27–37. [PubMed: 26725196]
- [25]. Azambuja AP, Simoes-Costa M, The connectome of neural crest enhancers reveals regulatory features of signaling systems, *Dev Cell* 56(9) (2021) 1268–1282 e6. [PubMed: 33852891] ** To identify the cis-regulatory regions which is Wnt dependent regulation of neural crest development, CRISPR-Cas9 was used to deplete putative enhancers in chick embryo neural crest cells.
- [26]. Kumar S, Hedges SB, A molecular timescale for vertebrate evolution, *Nature* 392(6679) (1998) 917–20. [PubMed: 9582070]
- [27]. Lindsey SE, Butcher JT, Yalcin HC, Mechanical regulation of cardiac development, *Front Physiol* 5 (2014) 318. [PubMed: 25191277]
- [28]. Yu F, Li R, Parks E, Takabe W, Hsiai TK, Electrocardiogram signals to assess zebrafish heart regeneration: implication of long QT intervals, *Ann Biomed Eng* 38(7) (2010) 2346–57. [PubMed: 20221900]
- [29]. Lee J, Cao H, Kang BJ, Jen N, Yu F, Lee CA, Fei P, Park J, Bohlool S, Lash-Rosenberg L, Shung KK, Hsiai TK, Hemodynamics and ventricular function in a zebrafish model of injury and repair, *Zebrafish* 11(5) (2014) 447–54. [PubMed: 25237983]
- [30]. Yalcin HC, Amindari A, Butcher JT, Althani A, Yacoub M, Heart function and hemodynamic analysis for zebrafish embryos, *Dev Dyn* 246(11) (2017) 868–880. [PubMed: 28249360]
- [31]. Vedula V, Lee J, Xu H, Kuo CJ, Hsiai TK, Marsden AL, A method to quantify mechanobiologic forces during zebrafish cardiac development using 4-D light sheet imaging and computational modeling, *PLoS Comput Biol* 13(10) (2017) e1005828. [PubMed: 29084212]
- [32]. Ho S, Chan WX, Phan-Thien N, Yap CH, Organ Dynamics and Hemodynamic of the Whole HH25 Avian Embryonic Heart, Revealed by Ultrasound Biomicroscopy, Boundary Tracking, and Flow Simulations, *Sci Rep* 9(1) (2019) 18072. [PubMed: 31792224]
- [33]. Lee J, Vedula V, Baek KI, Chen J, Hsu JJ, Ding Y, Chang CC, Kang H, Small A, Fei P, Chuong CM, Li R, Demer L, Packard RRS, Marsden AL, Hsiai TK, Spatial and temporal variations in hemodynamic forces initiate cardiac trabeculation, *JCI Insight* 3(13) (2018).
- [34]. Chen J, Ding Y, Chen M, Gau J, Jen N, Nahal C, Tu S, Chen C, Zhou S, Chang CC, Lyu J, Xu X, Hsiai TK, Packard RRS, Displacement analysis of myocardial mechanical deformation

(DIAMOND) reveals segmental susceptibility to doxorubicin-induced injury and regeneration, *JCI Insight* 4(8) (2019).

- [35]. Ding Y, Ma J, Langenbacher AD, Baek KI, Lee J, Chang CC, Hsu JJ, Kulkarni RP, Belperio J, Shi W, Ranjbarvaziri S, Ardehali R, Tintut Y, Demer LL, Chen JN, Fei P, Packard RRS, Hsiai TK, Multiscale light-sheet for rapid imaging of cardiopulmonary system, *JCI Insight* 3(16) (2018).
- [36]. Wang Z, Zhu L, Zhang H, Li G, Yi C, Li Y, Yang Y, Ding Y, Zhen M, Gao S, Hsiai TK, Fei P, Real-time volumetric reconstruction of biological dynamics with light-field microscopy and deep learning, *Nat Methods* 18(5) (2021) 551–556. [PubMed: 33574612] ** To improve quality and overcome the limitations of light-field microscopy imaging, view-channel-depth neural network with light-field imaging that provides a better reconstruction quality and less reconstruction artifacts than light-field microscopy, was approached and verified by imagings of neuronal activities in *Caenorhabditis elegans* and hemodynamics in zebrafish heart.
- [37]. Baek KI, Ding Y, Chang CC, Chang M, Sevag Packard RR, Hsu JJ, Fei P, Hsiai TK, Advanced microscopy to elucidate cardiovascular injury and regeneration: 4D light-sheet imaging, *Prog Biophys Mol Biol* 138 (2018) 105–115. [PubMed: 29752956]
- [38]. Fei P, Lee J, Packard RR, Sereti KI, Xu H, Ma J, Ding Y, Kang H, Chen H, Sung K, Kulkarni R, Ardehali R, Kuo CC, Xu X, Ho CM, Hsiai TK, Cardiac Light-Sheet Fluorescent Microscopy for Multi-Scale and Rapid Imaging of Architecture and Function, *Sci Rep* 6 (2016) 22489. [PubMed: 26935567]
- [39]. Fei P, Nie J, Lee J, Ding Y, Li S, Zhang H, Hagiwara M, Yu T, Segura T, Ho C-M, Zhu D, Hsiai T, Subvoxel light-sheet microscopy for high-resolution high-throughput volumetric imaging of large biomedical specimens, *Advanced Photonics* 1(1) (2019) 016002.
- [40]. White RM, Sessa A, Burke C, Bowman T, LeBlanc J, Ceol C, Bourque C, Dovey M, Goessling W, Burns CE, Zon LI, Transparent adult zebrafish as a tool for in vivo transplantation analysis, *Cell Stem Cell* 2(2) (2008) 183–9. [PubMed: 18371439]
- [41]. Chen XK, Kwan JS, Chang RC, Ma AC, 1-phenyl 2-thiourea (PTU) activates autophagy in zebrafish embryos, *Autophagy* 17(5) (2021) 1222–1231. [PubMed: 32286915] * An inhibitor of tyrosinase, 1-phenyl 2-thiourea (PTU), treatment suppress pigmentation in zebrafish embryo, whereas unexpectedly, PTU boosts autophagic flux in different zebrafish organs. This paper concerns using PTU to remove pigmentation in zebrafish embryo.
- [42]. Wang Y, Lu X, Wang X, Qiu Q, Zhu P, Ma L, Ma X, Herrmann J, Lin X, Wang W, Xu X, atg7-Based Autophagy Activation Reverses Doxorubicin-Induced Cardiotoxicity, *Circ Res* 129(8) (2021) e166–e182. [PubMed: 34384247]
- [43]. Wang Z, Ding Y, Satta S, Roustaei M, Fei P, Hsiai TK, A hybrid of light-field and light-sheet imaging to study myocardial function and intracardiac blood flow during zebrafish development, *PLoS Comput Biol* 17(7) (2021) e1009175. [PubMed: 34228702] ** This study observed the combination of light-field microscopy and light-sheet-fluorescence microscopy method achieve detecting the ventricular wall and blood flow movements simultaneously in zebrafish.
- [44]. Garcia-Canadilla P, Dejea H, Bonnin A, Balicevic V, Loncaric S, Zhang C, Butakoff C, Aguado-Sierra J, Vazquez M, Jackson LH, Stuckey DJ, Rau C, Stamparoni M, Bijmens B, Cook AC, Complex Congenital Heart Disease Associated With Disordered Myocardial Architecture in a Midtrimester Human Fetus, *Circ Cardiovasc Imaging* 11(10) (2018) e007753. [PubMed: 30354476]
- [45]. Alser M, Salman HE, Naija A, Seers TD, Khan T, Yalcin HC, Blood Flow Disturbance and Morphological Alterations Following the Right Atrial Ligation in the Chick Embryo, *Front Physiol* 13 (2022) 849603. [PubMed: 35492580] *In the paper, the authors performed the right atrial ligation surgery in chick embryo to mimic the hypoplastic right heart syndrome, however, there was no sever impact on blood flow and ventricular development.
- [46]. Lauridsen H, Gonzales S, Hedwig D, Perrin KL, Williams CJA, Wrege PH, Bertelsen MF, Pedersen M, Butcher JT, Extracting physiological information in experimental biology via Eulerian video magnification, *BMC Biol* 17(1) (2019) 103. [PubMed: 31831016]
- [47]. Ryvlin J, Lindsey SE, Butcher JT, Systematic Analysis of the Smooth Muscle Wall Phenotype of the Pharyngeal Arch Arteries During Their Reorganization into the Great Vessels and Its

Association with Hemodynamics, *Anat Rec (Hoboken)* 302(1) (2019) 153–162. [PubMed: 30312026]

- [48]. Haniffa M, Taylor D, Linnarsson S, Aronow BJ, Bader GD, Barker RA, Camara PG, Camp JG, Chedotal A, Copp A, Etchevers HC, Giacobini P, Gottgens B, Guo G, Hupalowska A, James KR, Kirby E, Kriegstein A, Lundeberg J, Marioni JC, Meyer KB, Niakan KK, Nilsson M, Olabi B, Pe'er D, Regev A, Rood J, Rozenblatt-Rosen O, Satija R, Teichmann SA, Treutlein B, Vento-Tormo R, Webb S, Human N Cell Atlas Developmental Biological, A roadmap for the Human Developmental Cell Atlas, *Nature* 597(7875) (2021) 196–205. [PubMed: 34497388] **This perspective paper presents a research direction how to study to understand tissue development by proposing the Human Developmental Cell Atlas project. Especially, the authors highlighted that multiomics including scRNA-seq and spatial sequencing are necessary to be parallel with 3D reconstruction by light-sheet microscopy methods.
- [49]. Lee J, Fei P, Packard RR, Kang H, Xu H, Baek KI, Jen N, Chen J, Yen H, Kuo CC, Chi NC, Ho CM, Li R, Hsiai TK, 4-Dimensional light-sheet microscopy to elucidate shear stress modulation of cardiac trabeculation, *J Clin Invest* 126(5) (2016) 1679–90. [PubMed: 27018592]
- [50]. Packard RRS, Baek KI, Beebe T, Jen N, Ding Y, Shi F, Fei P, Kang BJ, Chen PH, Gau J, Chen M, Tang JY, Shih YH, Ding Y, Li D, Xu X, Hsiai TK, Automated Segmentation of Light-Sheet Fluorescent Imaging to Characterize Experimental Doxorubicin-Induced Cardiac Injury and Repair, *Sci Rep* 7(1) (2017) 8603. [PubMed: 28819303]

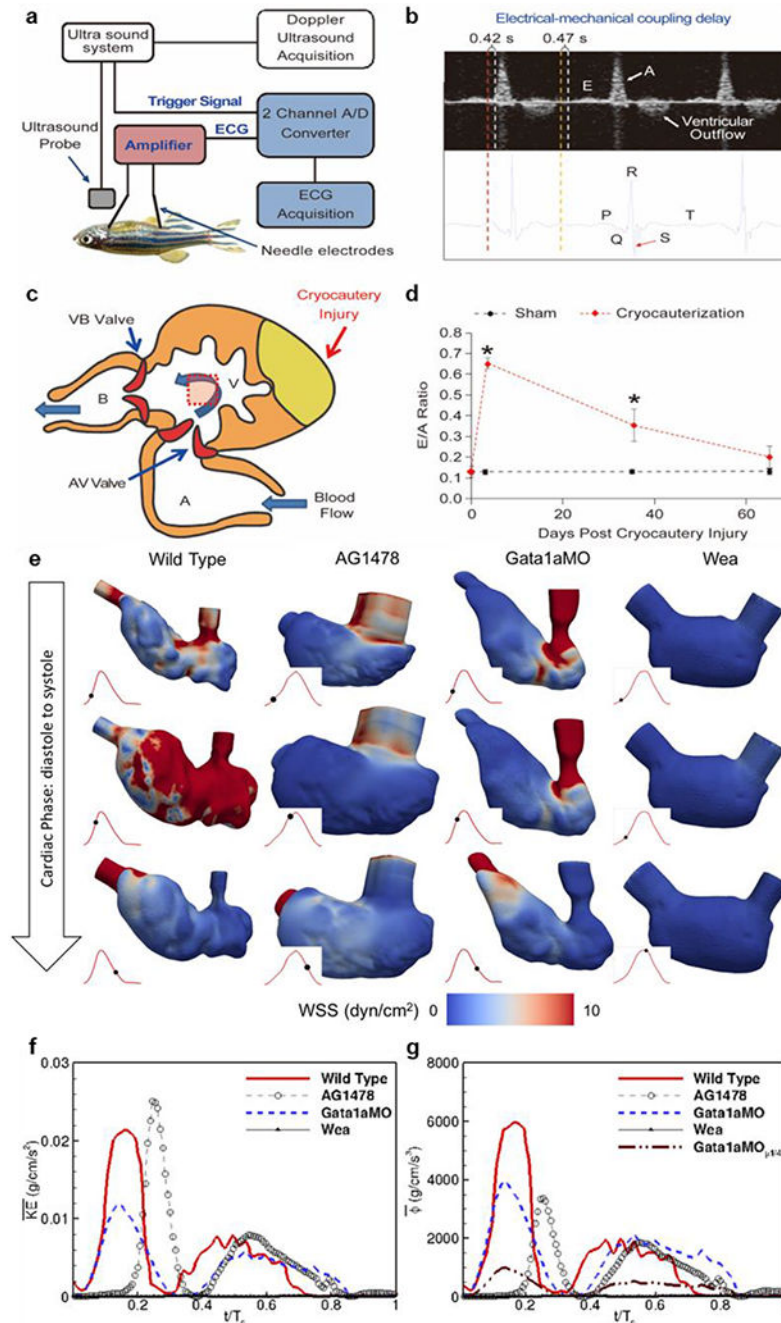


Fig. 1. μ ECG-gated PW Doppler to interrogate diastolic function and the effects of hemodynamic force and trabeculation on kinetic energy dissipation.

(a) The ultrasonic transducer is positioned ~ 6 mm above the fish heart. The micro-electrode is introduced laterally to the chest, and the reference electrode is positioned near the tail. When the Doppler recording is initiated, the system transmits a trigger signal to start ECG recording. (b) ECG-gated recording helps register the A-wave (P- on the ECG, red dotted line) and E-wave (ventricular relaxation, yellow). (c) The schematic diagram of the zebrafish heart illustrates ventricular apical cryoablation by liquid nitrogen. The red

dotted square indicates the position of the Doppler gated window upstream from the atrio-ventricular (AV) valve and downstream from the ventricular outflow tract (aortic valve). **(d)** Cryocauterization of the zebrafish ventricle significantly increased E/A ratios at 3 days post cryo-injury (dpc) and 35 dpc (* $p < 0.001$, $n=7$), which returned to the baseline value at 65 dpc. A: atrium; B: bulbous arteriosus; V: ventricle. **(e)** Endocardial wall shear stress (WSS) profiles are compared at different cardiac phases (rows) corresponding to early diastole, mid-diastole and mid-systole, between the wild type zebrafish embryos and in response to chemical and genetic treatments wild type, AG1478, *gata1a*MO, *wea*. The red line in each figure represents ventricular volume variation and the black dot identifies the corresponding instant during the cardiac cycle. All the phases are chosen to be at the same non-dimensionalized time with respect to the cardiac cycle duration (T_c) of each fish. This figure also illustrates the differences in ventricular morphology (volume and deformation) during the cardiac cycle for the chemically and genetically altered fish. **(f-g)** Comparison of **(f)** kinetic energy density, and **(g)** the rate of viscous dissipation per unit volume during the cardiac cycle, between the wild type zebrafish and in response to chemical (AG1478) and genetic (*gata1a*MO, *wea*) treatments.

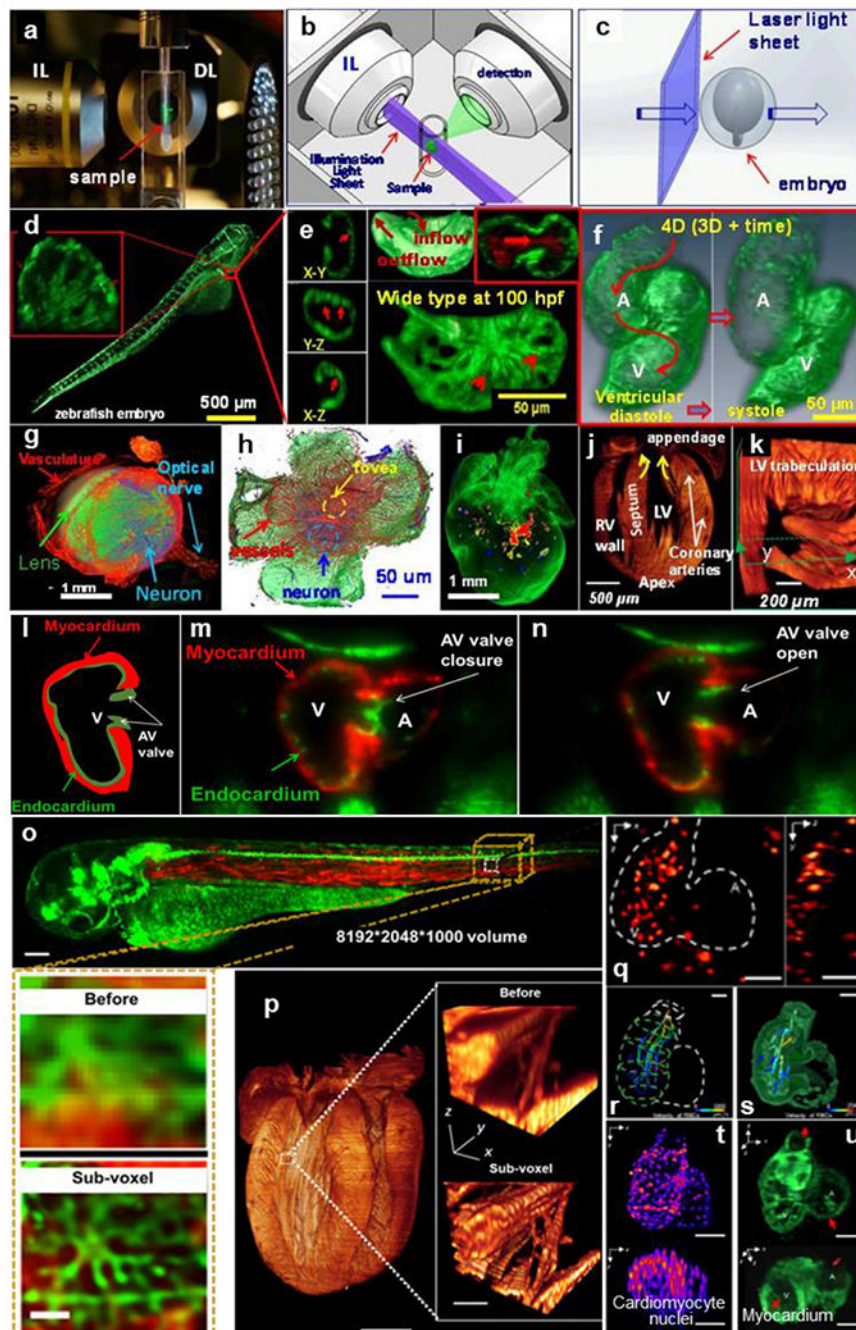


Fig. 2. Light-sheet and light-field systems in cardiac studies.

(a-k) Single illumination LSFM imaging. (a) The sample is positioned at the orthogonal intersection of the illumination lens (IL) and detection lens (DL). (b) A laser light-sheet is applied to rapidly illuminate the sample. The illuminated planes are orthogonally detected by the detection lens (DL). (c) A sheet of light transverses the embryo. (d) The entire 3-D embryo can be imaged. (e) 3-D images reveal the inflow and outflow tracts and endocardial trabecular ridges and grooves. (f) 4-D LSFM imaging and synchronization algorithm reconstruct systolic and diastolic structure at 120 hrs post fertilization. (g) 3-D

LSFM tracks the multi-channel fluorescent images of adult mouse ocular anatomy. **(h)** Adult mouse retinal vasculature and ganglia. **(i)** 3-D LSFM tracks the multi-channel fluorescent images of the cardiac progenitor lineage in an E7 neonatal rainbow mouse heart. Muscular ridges and trabeculae develop in the left atrial (LA) appendage. **(j)** 3-D Td tomato-labeled cardiomyocytes show the myocardium of the E7 heart. The yellow arrows point to the atrio-ventricular valves. **(k)** Apical trabeculation develops. **(l-n)** *In vivo* imaging of the AV valve movement. **(l)** A schematic of the AV valve leaflets and myocardium (cardiomyocyte light chain (*cmhc*)-labeled mCherry) and the endocardium (*flil*-labeled GFP). **(m-n)** AV valve leaflet **(m)** closure and **(n)** open at 100 fps. Scale bars: 200 μm [49, 50]. **(o-p)** SV-LSFM imaging. **(o)** A motor neuron/somite muscles in an *Tg(islet:gfp-mhcr:dsred)* embryo at 72 dpf. Scale bar: 100 μm and inset 20 μm . **(p)** An intact mouse heart at P1 exhibited endogenous autofluorescence. Scale bar: 1 mm and inset 50 μm . **(q-u)** Multiplex imaging cardiac hemodynamics in a beating zebrafish heart. Scale bars: 50 μm . **(q)** Maximum intensity projections (MIP) in x-y (left) and y-z (right) planes of one instantaneous volume of flowing RBCs. The dash lines indicate the heart. **(r)** Tracks of 19 single RBCs throughout the cardiac cycle. A static heart is outlined for reference. **(s)** Velocity map of two temporally adjacent volumes of RBCs during systole. **(t)** MIPs in x-y (top) and x-z (bottom) planes of one instantaneous volume of beating myocytes (mid-density GFP signals). **(u)** 3-D visualization of beating myocardium in a transient moment. The myocardium was densely labeled by GFP which shows continuous trabecular structures. Arrows indicate the inlet and outlet of cardiac pumping.

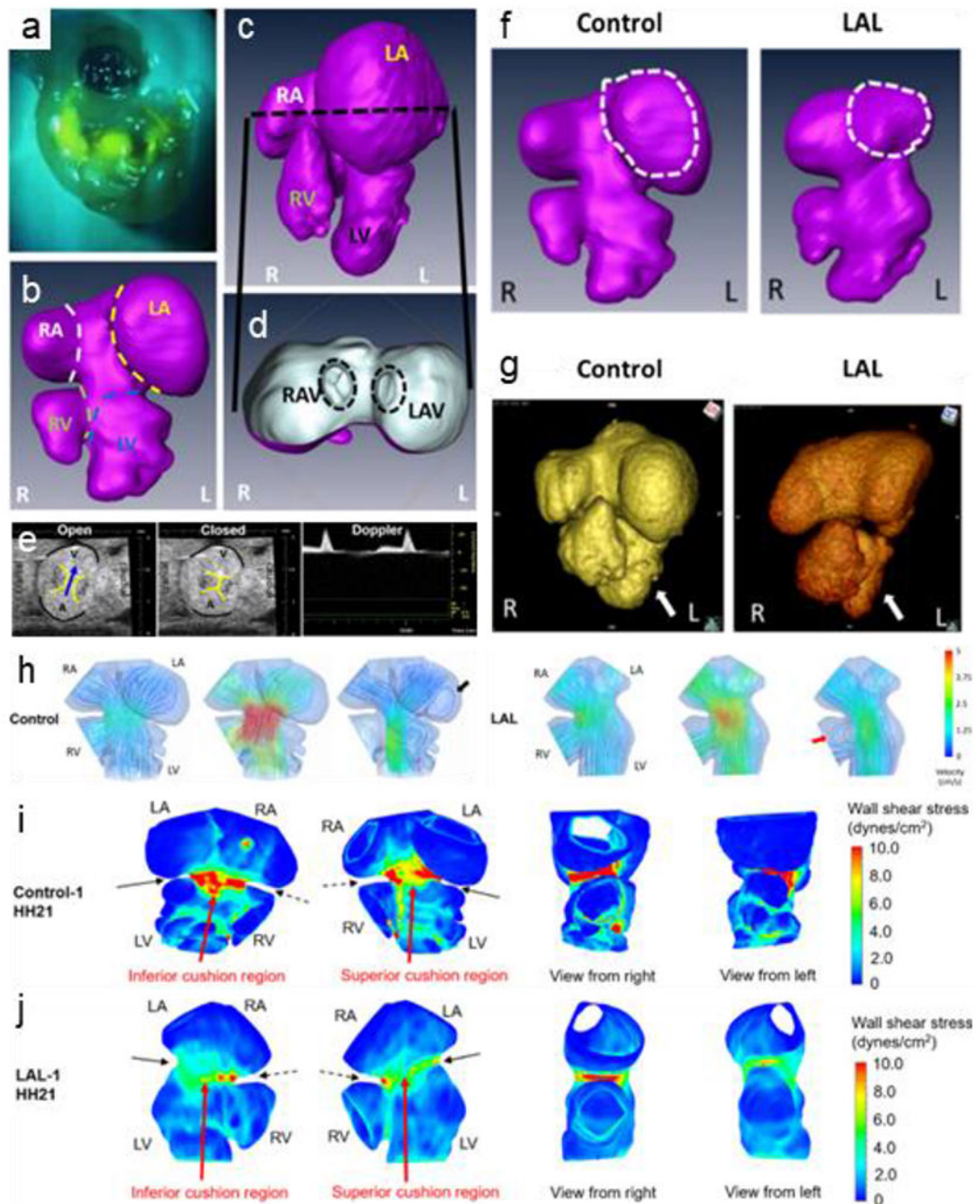


Fig. 3. Micro-CT and computational fluid modelling system in chick model.

(a) CT-dense contrast agent perfused through cardiovascular system for cast creation. (b-d) Micro-CT-generated 3D embryonic chicken heart. (b) Unseptated 3.5-day (HH21) heart. (c) Septated 7-day (HH30) heart. (d) Right and left AV canals revealed in cross-section of atria. (e) Echocardiography imaging for an HH21 embryo. B-mode images and Doppler velocity measurements for AV canal. In B-mode images, AVC is atrioventricular cushion. Arrow shows the blood flow direction. Edges of atrial and ventricular myocardium are highlighted in black. Edges of AVC are highlighted in yellow (f-g) Micro-CT geometries for control and

LAL embryos at **(f)** HH21 and at **(g)** HH30. **(h)** Velocity streamlines of HH21 LAL and control hearts at different phases of cardiac cycle. Black arrow shows the recirculation in the LA of control heart which is not present in LAL heart. Red arrow shows the redirection of flow to RV after the LAL interference **(i-j)** WSS distribution at peak AV flow velocity for HH21 control **(i)** and LAL **(j)** hearts.

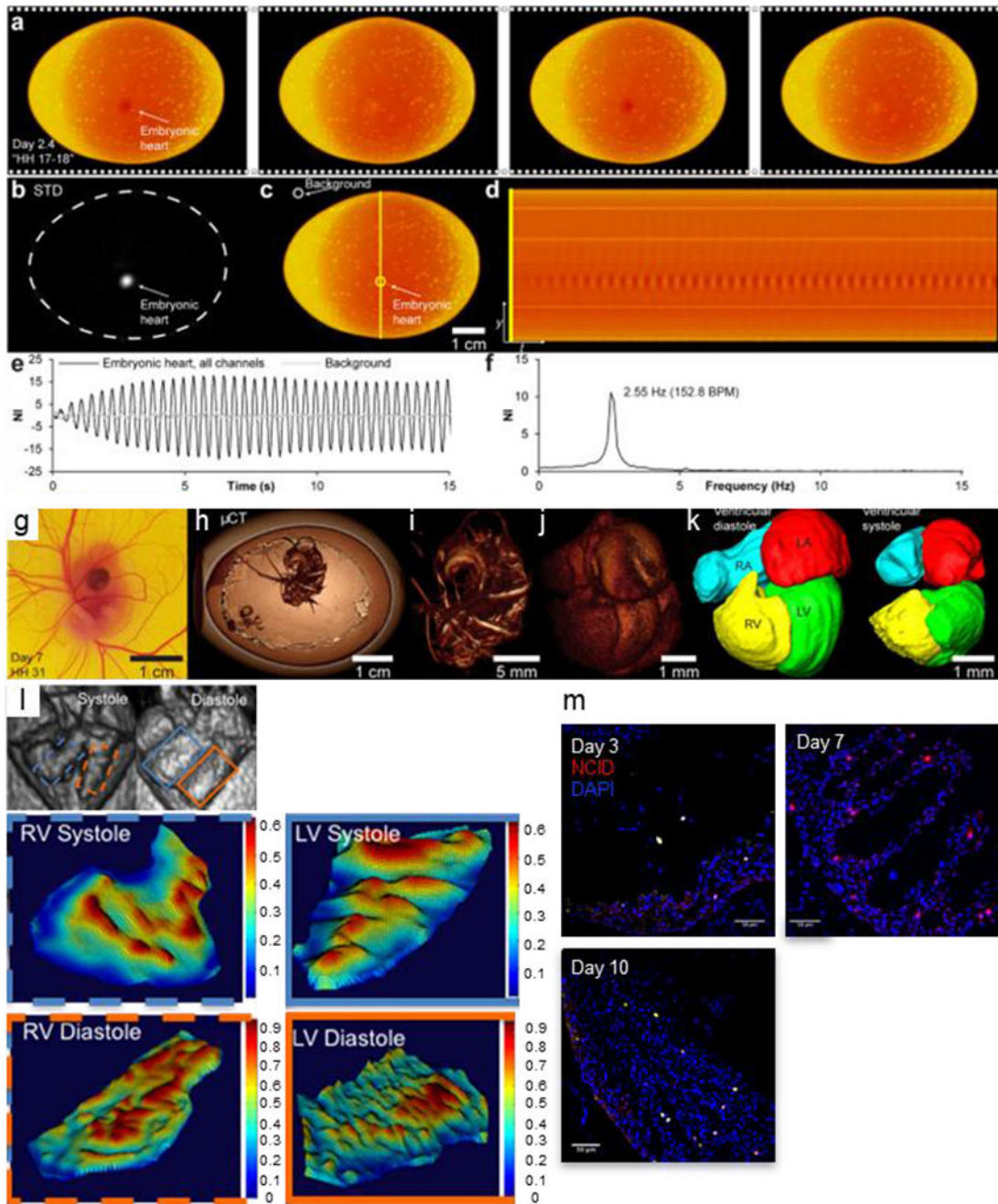


Fig. 4. Live prospective gated imaging of chick heart function by heart rate detection. (a) Four-frame time series showing color changes associated with the heartbeat in color-magnified video of embryonic chicken at day 2.4 in a candled. (b) Pixel-wise standard deviation (STD) of magnified video highlighting embryonic heart. (c-d) Image probes (c) and vertical scan line (d) over time showing temporal variation at embryonic heart intersection. (e-f) Embryonic heart and background signal development over time (e) and Fourier-transformed signal in the frequency domain (f). (g) Embryonic chicken on day 7. (h-i) 3-D rendering of embryonic chicken at day 7 from micro-CT imaging gated by the

magnified optical signal. Volumetric reconstruction of the heart and vascular system of the embryo in a resealed egg **(h-j)**, and segmentation of the heart chambers in diastole and systole **(k)**. **(l)** 4D Trabecular pattern analysis reveals unique trabecular orientations and strut thicknesses in each chamber, which change shape and orientation between Diastole and Systole. **(m)** Immunohistochemical staining of Notch intracellular domain (NICD) and DAPI in chick ventricles at day 3, 7, and 10.

Author Manuscript




Author Manuscript

Author Manuscript

Author Manuscript

Table 1.

Genetic vs. Mechanical perturbations among the animal models. LV: left ventricle, RV: right ventricle, RAL: Right atrial ligation, LAL: Left atrial ligation,

	Genetic perturbations				Mechanical perturbations	
	Transgenic lines for endocardial	Genetic manipulation to increase shear stress	Genetic manipulation to increase LV contraction	Genetic manipulation to change kinetic energy	RAL/LAL to alter RV/LV preload	Outflow track banding to increase RV/LV afterload
 Mouse embryo	●	●	●	●	●	●
 Chick embryo	●	●	●	●	●	●
 Zebrafish embryo	●	●	●	●	●	●

Author Manuscript

Author Manuscript

Author Manuscript

Author Manuscript